A R C H I V E S O F M E T A L L U R G Y A N D M A T E R I A L S
Volume 57 2012 Issue 2
DOI: 10.2478/v10172-012-0043-2

B. ERTUĞ*, T. BOYRAZ**, O. ADDEMİR***

# INVESTIGATION OF THE ELECTRICAL CONDUCTIVITY AND HUMIDITY SENSITIVITY CHARACTERISTICS OF $BaTiO_3$ CERAMICS WITH PMMA ADDITIVE

# BADANIE PRZEWODNOŚCI ELEKTRYCZNEJ I CHARAKTERYSTYKA CZUŁOŚCI NA WILGOTNOŚĆ CERAMIKI $BaTiO_3$ Z DODATKIEM PMMA

Humidity sensing is a requirement for human comfort and several industrial processes. There are two main types of humidity-sensing mechanisms. One of them is the protonic sensor which utilizes ionic conductivity due to water physisorption or capillary condensation in micropores. The semiconductor sensors use the changes in electronic conductivity due to water chemisorption. In this study, an ionic type of sensor was fabricated. Barium titanate based ceramic humidity sensors made with PMMA(Polymethyl metacrylate) as the PFA (Pore-forming agent) were investigated. All compositions included 0.18 wt. % of $La_2O_3$ and three different PMMA contents. The green compacts were heated at 1200-1500°C for 2-6 h. in air and then furnace cooled. The fundamental characteristics of ceramic humidity sensors, electrical conductivity and humidity sensitivity were determined and discussed in relation to microstructural features, porosity, phase analysis and grain size data. The experimental results of conductivity measurements were evaluated in terms of practical sensor applications.

*Keywords*: Barium titanate, microstructure, electrical conductivity, humidity sensitivity

Pomiar wilgotności jest istotny dla ludzkiej wygody i wielu procesów przemysłowych. Istnieją dwa główne typy mechanizmów wykrywania wilgoci. Jednym z nich jest czujnik protonic, który wykorzystuje przewodnictwo jonowe dzięki fizykosorpcji wody lub kondensacji kapilarnej w mikroporach. Czujniki półprzewodnikowe wykorzystują zmiany przewodnictwa elektrycznego ze względu na chemisorpcję wody. W ramach niniejszej pracy, zbudowany został czujnik jonowy. Badane były ceramiczne czujniki wilgotności oparte o tytanian baru z dodatkiem PMMA (polimetakrylan metakrylanu) jako czynnika tworzenia porów. Wszystkie badane składy zawierały 0,18%.wag $La_2O_3$ i trzy różne zawartości PMMA. Zielone pakiety ogrzewano w temperaturze 1200-1500°C przez 2-6 godzin w powietrzu, a następnie studzono razem z piecem. Podstawowe cechy ceramicznych czujników wilgotności, przewodność elektryczna i wrażliwość na wilgotność zostały określone i omówione w odniesieniu do cech mikrostruktury, porowatości, analizy fazowej i danych o wielkości ziarna. Eksperymentalne wyniki pomiarów przewodności były oceniane w kategoriach praktycznych zastosowań czujników.

## 1. Introduction

Humidity sensors are a part of daily life comfort and several industrial processes. There is a number of materials that can be used as humidity sensing elements. Ceramic type humidity sensors are classified into ionic, electronic, capacitive and solid-electrolyte types based mechanisms. Two main mechanisms can be grouped as protonic and semiconductor type of sensing. The conduction carriers of the sensor in the humid atmosphere are ions and electrons. For the ionic or protonic type of sensors, the source of the electrical conductivity are the ions as the dominant conduction carrier. Ionic conductivity in resistive or ionic type of humidity sensors depends on water absorbtion. On the as-sintered surface of the metal oxide based humidity-sensing element, chemical and physical absorbtion of water molecules take place during the exposure to humid environment. On the other hand, capillary condensation in the micropores of ceramics also contributes to total electrical conductivity[1–5]. Thus a controlled amount of porosity is required for the humidity sensing ceramics.

Ceramics, in particular metal oxides, have advantages for humidity sensing applications in terms of their mechanical strength, their resistance to chemical attack and their thermal and physical stability. Perovskites

* GEDIK UNIVERSITY, DEPARTMENT OF METALLURGICAL AND MATERIALS ENGINEERING, 34876 YAKACIK-KARTAL, ISTANBUL,TURKEY
** CUMHURIYET UNIVERSITY, DEPARTMENT OF METALLURGICAL AND MATERIALS ENG., SIVAS,TURKEY
*** ISTANBUL TECHNICAL UNIVERSITY, DEPARTMENT OF METALLURGICAL AND MATERIALS ENG., ISTANBUL, TURKEY

are promising materials for humidity sensing applications. Perovskite denotes a group of crystal structures, whose basic chemical formula follows the pattern $ABO_3$, in which the basic unit is a primitive cube, with the A-cation in the cube center, the B-cations on the corners and the anion, commonly oxygen, in the centres of the face edges[6–8]. In the present study, a spesific polymer was used for the formation of controlled porosity in barium titanate based ceramic sensors. Low amounts of PMMA (Polymethyl metacrylate) were added and powder preparation was carried out by mixed solid oxide method. The effects of porosity, content of PFA (Pore-forming agent) and sintering parameters on the electrical conductivity of the barium titanate based ceramics were investigated. The humidity sensitivity graphs were obtained by the ratio of electrical resistivity in air to electrical resistivity in humid environment.

## 2. Experimental procedure

Barium titanate ceramics were prepared by using the $BaCO_3$ and $TiO_2$ raw materials. The compositions studied consist of 0.18 wt.% of $La_2O_3$. The compositions containing 1, 1.75 and 2.5 wt. of PMMA (Polymethyl metacrylate) were coded as BTLP-1, BTLP-2 and BTLP-3, respectively. The mixture of powders were ball-milled in acetone for 24 h in a plastic jar using $ZrO_2$ as the grinding media. The ball-milled slurries were dried at 100°C in an oven for 30 min. Afterwards, PMMA was added in another ball-milling step at a rate of 90rpm. The powders were pressed into bars with dimensions of 15×12×7mm using cold pressing. Prior to sintering, BTLP compositions were subjected to binder removal at one step using thermal pirolysis. The binder removal was done at a heating rate of 1°C/min. on alumina plates up to 650°C for 2h. using Protherm binder removal furnace. The green compacts were heated at 1200-1500°C for 2-6 h. in air and then furnace cooled. The crystalline structure of the as-sintered ceramics was analyzed with X-ray diffraction (XRD) (Rigaku DMAX 2500) using Co $K_\alpha$ radiation within arrange of $2\theta$ = 20°-80°. The microstructure of the as-sintered ceramics was examined using a scanning electron microscope (SEM) (JEOL 5600). The grain size of the as-sintered ceramics was measured by lineal interception method. The porosity of the ceramics was measured using Archimedes method. The electrical resistance values were measured by a standard multimeter (Digital Multimeter DY-64) using 2-probe measurement method under humid environment (Heraeus/Vötsch-HC 4033).

## 3. Results and discussion

The microstructures of the as-sintered samples are shown in Fig. 1. PMMA addition resulted in a slight grain refinement. After sintering at 1500°C for 6h., the grain size of BTLP-1 was 14.87 $\mu$m whereas the grain size of BTLP-3 was 13.75 $\mu$m. Also at lower sintering temperatures, PMMA addition caused a grain size inhibition. The grain sizes of BTLP-1 and BTLP-3 were 5.41 $\mu$m and 5 $\mu$m, respectively after sintering at 1200°C for 2h.

After sintering at 1500°C, the relative density of the as-sintered samples increased greatly. The pore elimination was present for all the sintering durations at 1500°C. This could be explained by the rapid increase in the grain growth kinetics of the samples when sintered up to 1500°C.

At lower sintering temperatures (except 1500°C) SEM images showed uniformly distributed pores in the matrix. Spaces were observed between the pores and intergranular pore morphology (Fig.1a) was present. However, after sintering at 1500°C, porosity was eliminated and grain size increased significantly.

Fig. 2 and Fig. 3 show XRD diagrams of the samples sintered at 1200°C. As the sintering duration increased from 2h. to 6h., the intensity of the XRD diagram increased. This was valid for all the sintering temperatures studied. (101) plane reflection was observed in Fig. 2 and 3, which has the maximum intensity at $2\theta$ = 36.701° and plane distance was 2.8412A°. In Fig. 2 and 3, a split peak was observed at $2\theta$ =52.595 and 53.220°, that correspond to (002) and (200) plane reflections, which is not observed in cubic symmetry of barium titanate and was used for the determination of tetragonal and cubic crystal structures. The plane distances of (002) and (200) reflections were determined by JCPDS card number 05-0626 as 2.0190 and 1.9970A°, respectively. Since all the compositions studied consist of a constant amount of $La_2O_3$, split peaks of tetragonal barium titanate gradually merged upon doping. This could be explained by the modification of crystal symmetry of tetragonal phase. Following the doping of barium titanate ceramics, a pseudo-cubic crystal symmetry formed. The reason for the merging of peaks could be the internal stresses formed via doping process. However, the amount of doping was not sufficient to transform room-temperature tetragonal barium titanate phase to cubic symmetry.

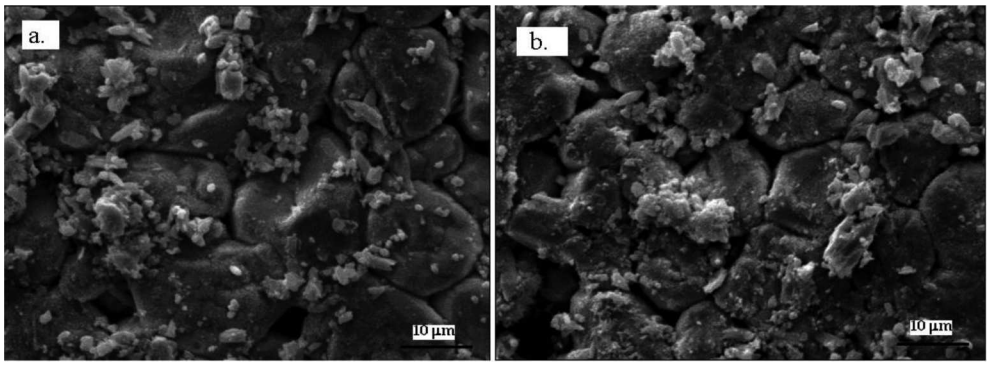


Fig. 1. SEM images for PMMA-containing (a) BTLP-1 and (b) BTLP-3 compositions sintered at 1500°C for 6h

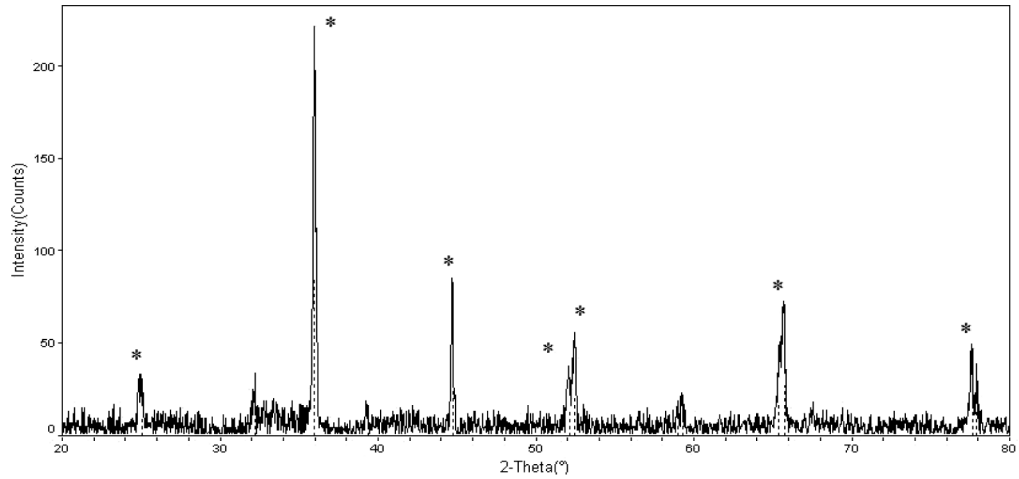


Fig. 2. XRD diyagram of barium titanate ceramics sintered at 1200°C for 2h., * denotes tetragonal phase

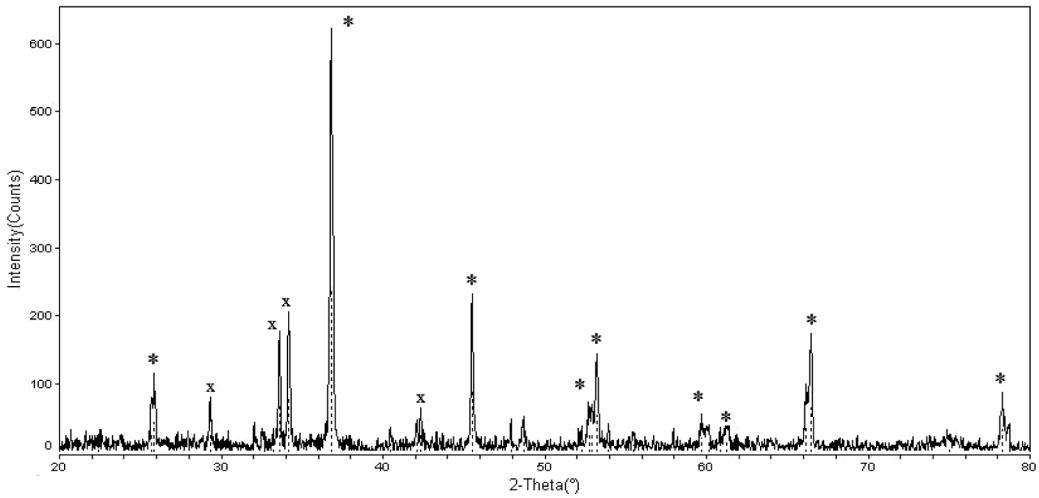


Fig. 3. XRD diyagram of barium titanate ceramics sintered at 1200°C for 6h., * denotes tetragonal and x unknown phase

It was clear that all the as-sintered ceramics showed a tetragonal perovskite structure, whatever PMMA content was. As a result, room temperature crystal structure of porous $BaTiO_3$ ceramics did not depend on the addition, or the amount of the pore-forming agent. On the other hand, PMMA added compositions did not contain residual carbon (invisible as XRD reflections) besides barium titanate phase. XRD peaks of BTLP-3 composition containing 2.5%wt. PMMA did not show considerable shifting in comparison to BTLP-1 and BTLP-2 compositions. There was no evolution of a secondary phase due to the existance of PMMA addition. It was

concluded that all the compositions studied contained variable percentages of porosity with a single perovskite $BaTiO_3$ phase.

The grain size vs. sintering temperature graph was given in Fig. 4. The grain sizes of BTLP-1 were 4.5 and 12.3 $\mu$m when sintered at 1200 and 1500°C, respectively. There was a great change in the grain sizes when sintered at minimum and maximum sintering temperatures. After sintering at 1500°C, the grain growth was evident. After sintering at 1200°C for 6h., the grain size decreased from 5.41 to 4.5 $\mu$m with the addition from 1 to 2.5wt. of PMMA. The largest grain size which was measured at the maximum sintering temperature was 14.87 $\mu$m, which was measured for BTLP-1 composition which contains 1 wt. of PMMA.

The porosity vs. sintering temperature graph was shown in Fig. 5. The porosity percentage vs. sintering temperature and PMMA content relationships were expressed as the eq. (1). The coefficients of the following quadratic equation was calculated to be $\alpha$ $5.91\times10^{2}$, $\beta$ $-7.46\times10^{-1}$, $\gamma$ $1.35\times10^{1}$, $\delta$ $2.4\times10^{-4}$, $\phi$ $-6.99\times10^{-1}$ and $\theta$ $-6.29\times10^{-3}$ for 2h.

$$\text{Porosity}(\%) = \alpha + \beta x T + \gamma x(\text{PMMA}\%) + \delta x T^2 + \phi x(\text{PMMA}\%)^2 + \theta x T x(\text{PMMA}\%) \quad (1)$$

According to eq. (1), after sintering at 1200°C as PMMA content increases from 1 to 2.5 wt.%, the porosity increases from 45% to 50.6%. These calculations were also confirmed by experimental results. By using the eq. (1), appropriate sintering parameters and PMMA content could be calculated for a desired porosity.

The transfer function curves for barium titanate ceramics (which contain PMMA) was given in Fig. 6 and Fig. 7. In Fig. 6.a, transfer function of the sample is an exponential curve. The maximum conductivity was $10^{-2.5}$S/m. and it was measured for BTLP-3 which was

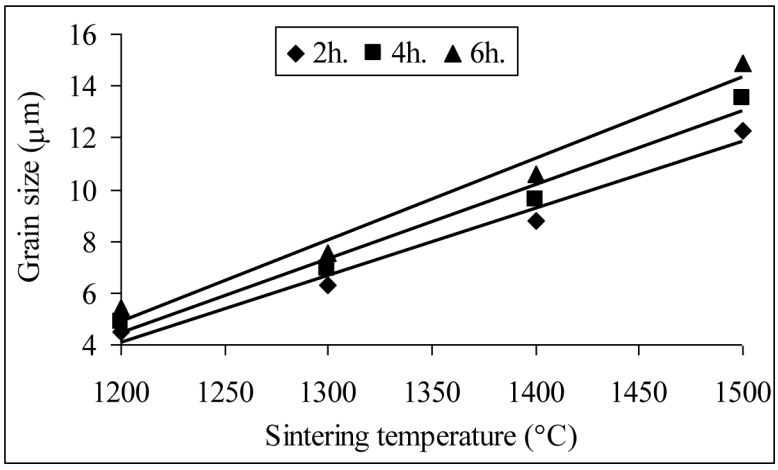


Fig. 4. Grain size vs. sintering temperature graphs for BTLP-1

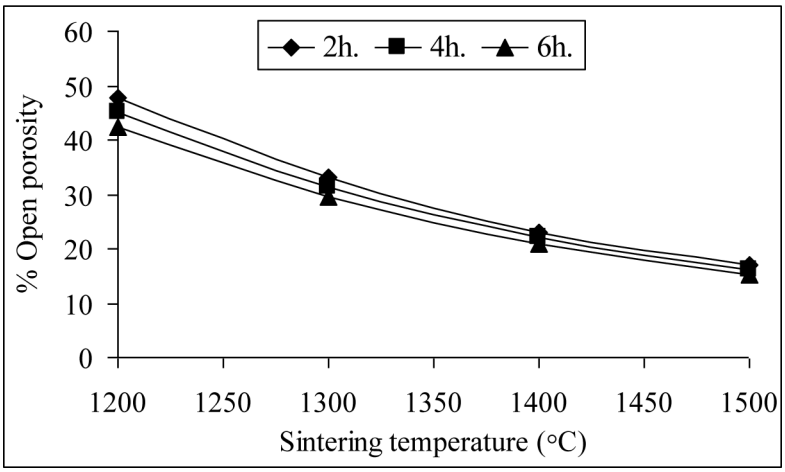


Fig. 5. Porosity vs. sintering temperature graphs for BTLP-1

sintered at 1200°C. Both BTLP-1 and BTLP-3 had a saturation limit on their transfer functions. The electrical conductivity vs. relative humidity for both of the samples were high. However, the existance of a saturation limit and lack of linearity above a certain relative humidity makes it difficult to use these samples for sensor applications despite their high conductivity.

The maximum electrical conductivity was determined to be $10^{-3.8}$S/m for the samples which were sintered at 1300°C for 2-6h. There is no saturation limit for the samples which were sintered at 1300°C. This is beneficial for humidity sensing. The linearity characteristic is high and the highest correlation factor, $R^2$ is 0.9978 for BTLP-1 which was sintered at 1300°C. When the sintering temperature was raised from 1300 to 1400°C, linearity characteristic degraded. The maximum conductivity after sintering at 1400°C was $10^{-4.75}$S/m. After sintering at 1500°C, linearity characteristic of the transfer functions degraded further and a dead band region was present. The maximum conductivity after sintering at 1500°C was $10^{-5.25}$S/m. The dead band region was up to 40% of relative humidity for BTLP-1. BTLP-3 did not show a dead band region but electrical conductivitivies were low and linearity characteristic was poor. The sintering temperature was the main parameter which determined the characteristic of the transfer functions.

Humidity sensitivity vs. relative humidity graphs were given in Fig. 8 and Fig. 9. Each value in the curves represents a ratio of the electrical resistance measured in air to the electrical resistance measured under humid environment. There was increase in the humidity sensitivity up to 80% of relative humidity. After 80%, increase in the humidity sensitivity was less for the samples which were sintered at 1200°C. For the samples sintered at 1300°C, the maximum humidity sensitivity was 1.9, which means sensitivity increased approximately in the order of 100 when sample exposed to a relative humidity of 98%. The samples which were sintered at

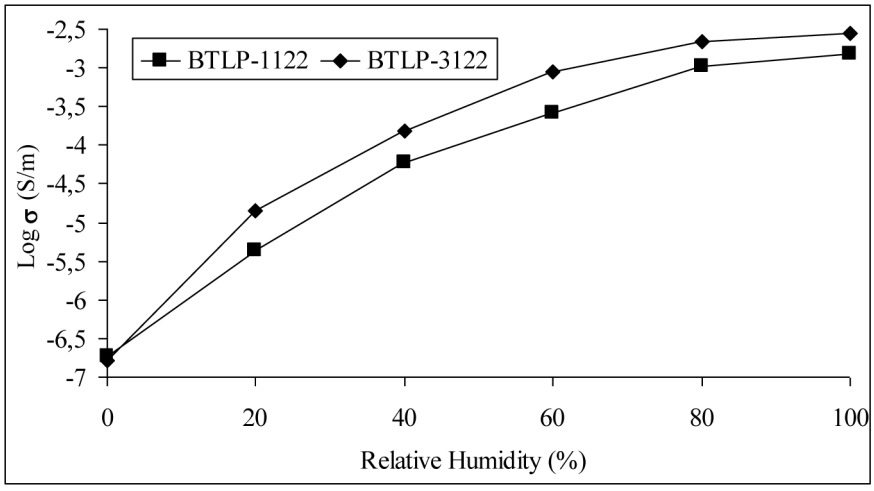


Fig. 6. Transfer function curves for barium titanate ceramics sintered at 1200°C

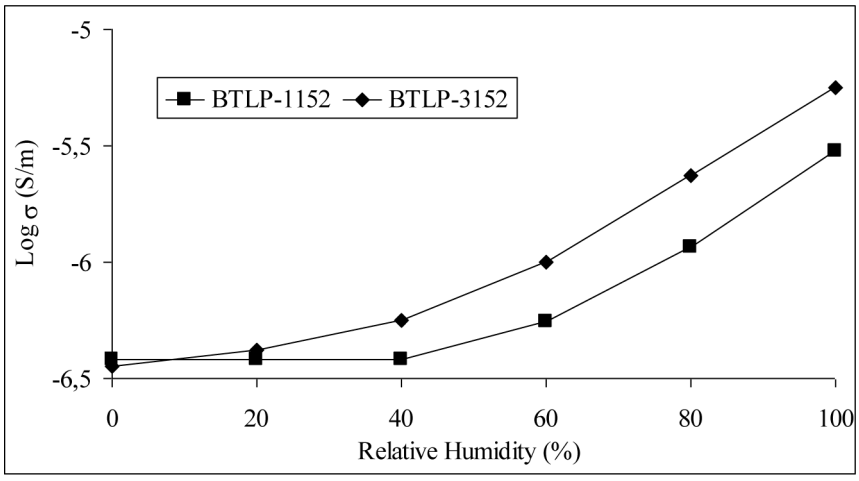


Fig. 7. Transfer function curves for barium titanate ceramics sintered at 1500°C

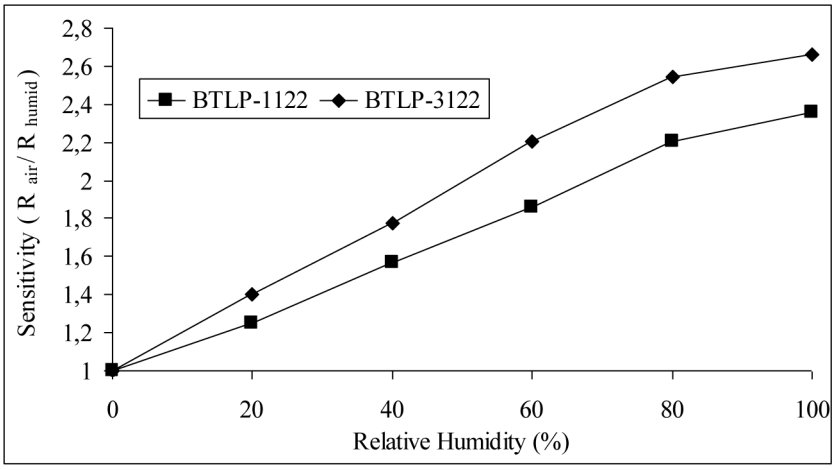


Fig. 8. Humidity sensitivity curves for barium titanate ceramics sintered at 1200°C

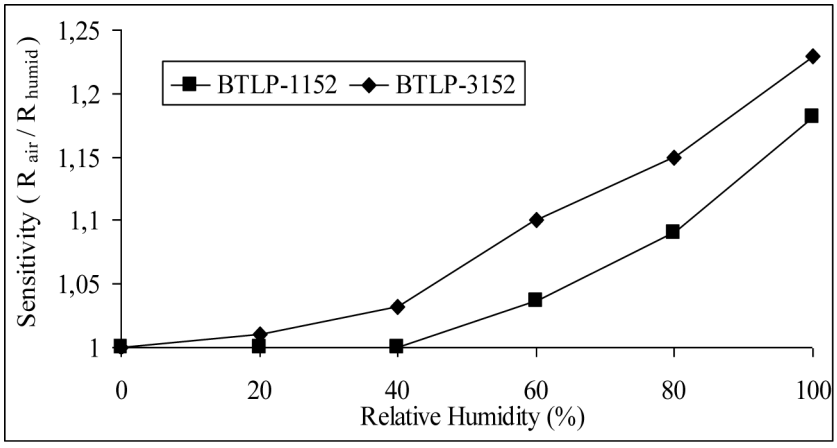


Fig. 9. Humidity sensitivity curves for barium titanate ceramics sintered at 1500°C

1500°C had a dead band region where humidity sensitivity is equal to 1.

## 4. Conclusion

The effects of PMMA (polymethyl metacrylate) additions on the microstructure and humidity sensitivity of barium titanate ceramics were examined. Porosity and microstructural studies were done for the samples which contain PMMA as the pore-forming agent. It was observed that there is no evolution of a secondary phase due to the existance of PMMA. As-sintered ceramics studied showed a tetragonal perovskite structure. As PMMA content increased, grain size values decreased slightly. Porosity percentage changes depending on the content of PMMA could be evaluated as the only parameter to affect electrical conductivity under humid environment. It was concluded that porous barium titanate ceramics can be used effectively for humidity sensing applications.

REFERENCES

[1] E.M. Sterling, Ashrae Winter Meeting **91**, 611-621 (1985).
[2] P.R. Morey, Ashrae Transactions **92**, 420-431 (1986).
[3] V. Matko, D. Donlagic, Sensors and Actuators **A 61**, 331-334 (1997).
[4] M. Takahashi, M. Fuji, KONA **20**, 84-97 (2002).
[5] G. Tschulena, A. Lahrmann, Sensors Applications, Sensors in Household Appliances (John Wiley and Sons, 2003) Chap.5 16.
[6] N. Setter, R. Waser, Acta Mater. **48**, 151-178 (2000).
[7] N. Setter, J. of the European Ceramic Society **21**, 1279-1293 (2001).
[8] E. Matsushita, A. Tanase, Solid State Ionics **97**, 45-50 (1997).

*Received: 10 September 2011.*